



## On Sampling fractions and electron shower shapes

Alexander Peryshkin<sup>1</sup> and Rajendran Raja<sup>2,\*</sup>

<sup>1</sup>*AT&T Services, Inc., 225W Randolph Avenue, 30A, Chicago, Il 60606*

<sup>2</sup>*Fermi National Accelerator Laboratory,  
P. O. Box 500, Batavia, IL 60510*

(Dated: December 29, 2011)

### Abstract

We study the usage of various definitions of sampling fractions in understanding electron shower shapes in a sampling multilayer electromagnetic calorimeter. We show that the sampling fractions obtained by the conventional definition (I) of (average observed energy in layer)/ (average deposited energy in layer) will not give the best energy resolution for the calorimeter. The reason for this is shown to be the presence of layer by layer correlations in an electromagnetic shower. The best resolution is obtained by minimizing the deviation from the total input energy using a least squares algorithm. The “sampling fractions” obtained by this method (II) are shown to give the best resolution for overall energy. We further show that the method (II) sampling fractions are obtained by summing the columns of a non-local  $\lambda$  tensor that incorporates the correlations. We establish that the sampling fractions (II) cannot be used to predict the layer by layer energies and that one needs to employ the full  $\lambda$  tensor for this purpose. This effect is again a result of the correlations.

PACS numbers: 14.20.-c, 14.40.Aq, 14.60.-z

---

\*Electronic address: [raja@fnal.gov](mailto:raja@fnal.gov)

## I. SAMPLING FRACTION DEFINITION METHOD I

We define the inverse sampling fraction  $\mu_I^k$  in method I as the average deposited energy  $D^k$  in layer k divided by the average live energy  $L^k$  in liquid argon in layer k, averaged over a sample of electrons of fixed incident energy. The deposited energy includes energy in Uranium plates, energy in dead material and the liquid argon gaps belonging to that layer.

$$\mu_I^k \equiv \langle D^k \rangle / \langle L^k \rangle \quad (1)$$

where  $\langle \rangle$  denotes average over events. Using this definition, we can calculate the total deposited energy event by event and also the layer by layer deposited energy as a function of the observed live energies.

$$D^{tot} = \sum_k \mu_I^k L^k \quad (2)$$

and the layer by layer deposited energies are

$$D_k = \mu_I^k L^k \quad (3)$$

Table (I) shows the inverse sampling fractions  $\mu_I^k$  for the 4 EM layers and the 1st layer of a hadronic calorimeter (FH1) which acts as a leakage detector. The numbers are obtained from a full plate simulation of the calorimeter using Geant 3.11 for 10 GeV/c and 100 GeV/c electrons.

It can be seen that the inverse sampling fraction increases as the shower proceeds. In particular, the ratio of the  $\mu_I$  to the inverse sampling fraction determined using minimum ionizing particles shows this effect in the second row of table (I)). This is due to mean free path of the average particle in the shower becoming comparable to the Uranium plate thickness, resulting in an increasing amount of tracks terminating in Uranium and not making it into the argon. The effect is particularly noticeable in FH1 where the shower is in the process of terminating. Using,  $\mu_I$ , we calculate the  $D^{tot}$  and also individual  $D^k$ . Figure (1) is the total energy  $D^{tot}$  calculated using this method. The overall energy resolution in this method is roughly  $40\%/\sqrt{(E)}$ . Figure (2) shows the difference between the calculated

<i>Momentum</i>	<i>EM1</i>	<i>EM2</i>	<i>EM3</i>	<i>EM4</i>	<i>FH1</i>
	$\mu_I^1$	$\mu_I^2$	$\mu_I^3$	$\mu_I^4$	$\mu_I^5$
10.0	12.2	12.3	16.1	19.3	139.6
	$\mu_I^1/MIP^1$	$\mu_I^2/MIP^2$	$\mu_I^3/MIP^3$	$\mu_I^4/MIP^4$	$\mu_I^5/MIP^5$
10.0	0.39	1.08	1.43	1.56	8.1
	$\mu_I^1$	$\mu_I^2$	$\mu_I^3$	$\mu_I^4$	$\mu_I^5$
100.0	10.4	11.2	15.0	18.4	59.9
	$\mu_I^1/MIP^1$	$\mu_I^2/MIP^2$	$\mu_I^3/MIP^3$	$\mu_I^4/MIP^4$	$\mu_I^5/MIP^5$
100.0	0.34	0.98	1.34	1.49	3.47
<i>MIP</i>	31.05	11.4	11.23	12.34	17.24

TABLE I: Inverse sampling fractions method I for 10 GeV/c and 100 GeV/c electrons. Also shown are the inverse sampling fractions estimated using Minimum Ionizing particles (MIP) and the ratio of Method I/MIP

event by event quantities  $D^k$  using method I and the Monte Carlo measured  $D^k$  for the various layers.

## II. SAMPLING FRACTION DEFINITION METHOD II

In order to optimize the resolution, it is usual to minimize the sum of squares of the difference between the calculated total energy and the input total energy event by event. We minimize  $S^2$  defined as

$$S^2 \equiv \sum_{events} (D^{tot} - \sum_k \mu_{II}^k L^k)^2 \quad (4)$$

To minimize,

$$\frac{dS^2}{d\mu_{II}^j} = -2 \sum_{events} (D^{tot} - \sum_k \mu_{II}^k L^k) L^j = 0 \quad (5)$$

Averaging over the number of events, this yields

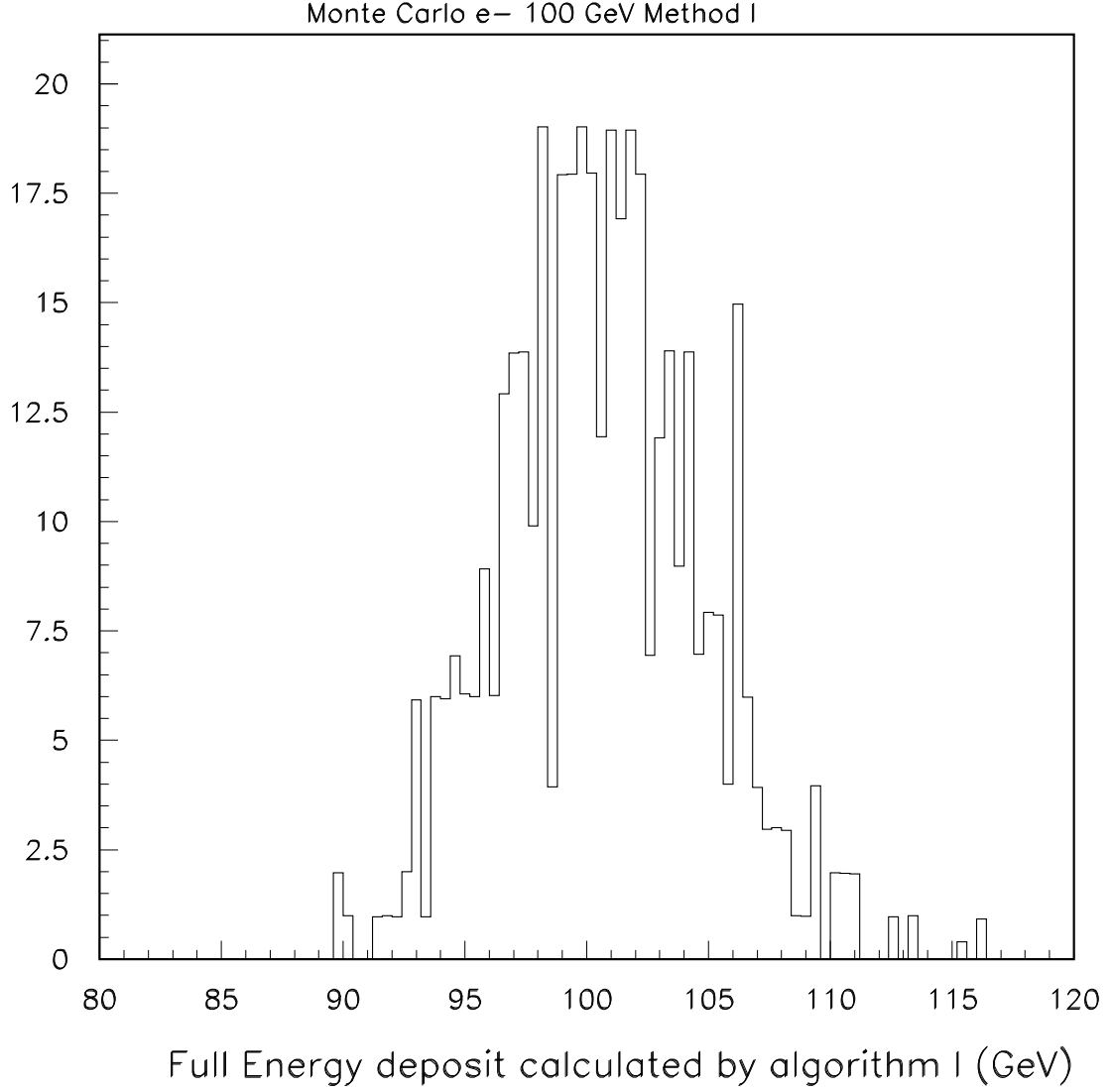


FIG. 1: Total energy of electron showers calculated using method I. The mean reconstructed energy is 100.0 GeV and the rms is 4.095 GeV

$$\langle D^{tot} L^j \rangle = \sum_k \mu_{II}^k \langle L^k L^j \rangle \quad (6)$$

with the matrix  $M^{jk} \equiv \langle L^j L^k \rangle$ , we can solve for  $\mu_{II}$

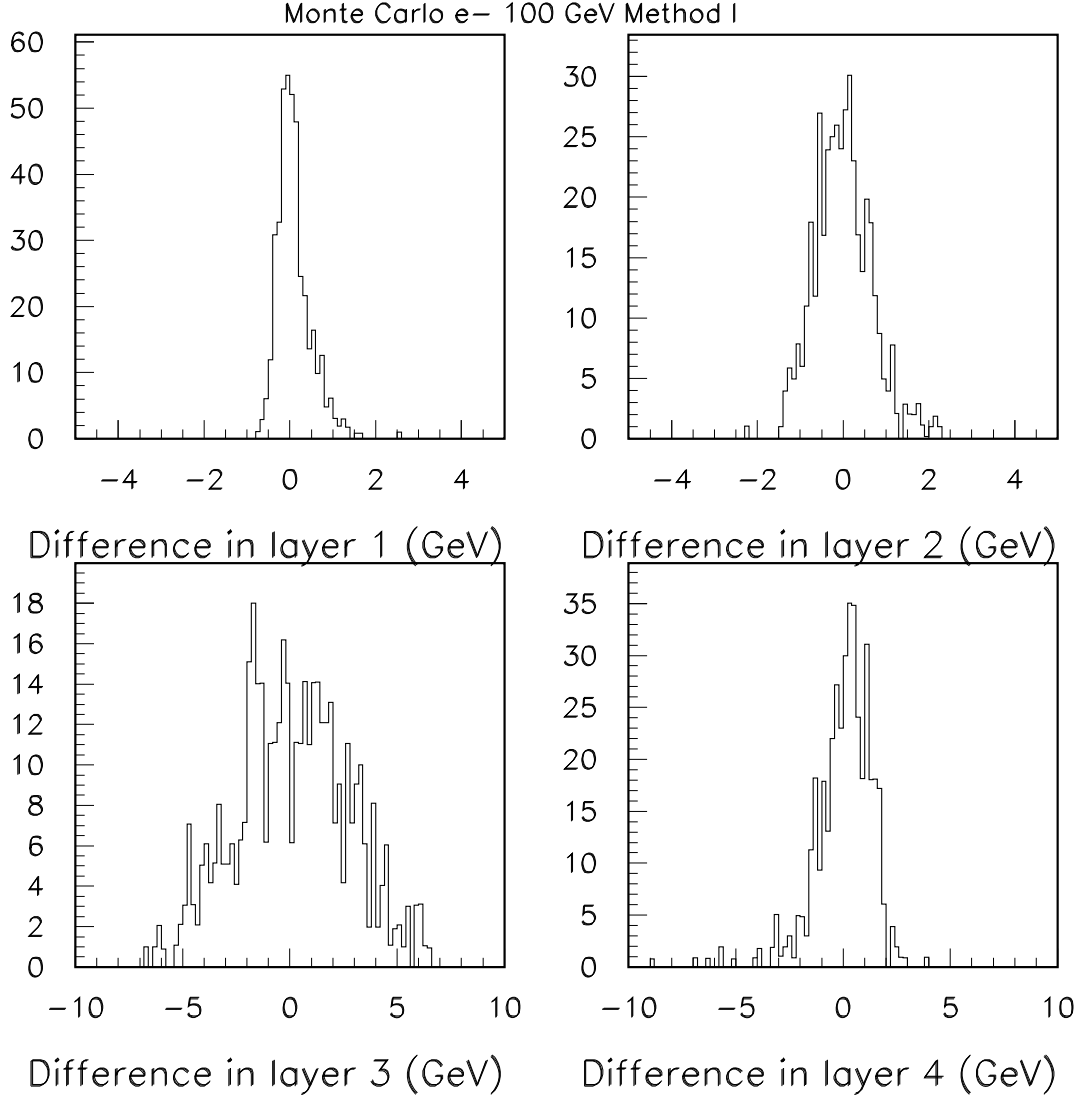


FIG. 2: Difference in energy (Monte Carlo -predicted ) layer by layer using method I. Layer 1 has mean,RMS of (0.59E-3 GeV and 0.407 GeV), layer 2 ( -0.11E-2 GeV and 0.56 GeV), layer 3 (-0.12E-2 GeV and 3.5 GeV) and layer 4 (-0.7E-3 GeV and 1.43 GeV)

$$\mu_{II}^a = \sum_j \langle D^{tot} L^j \rangle (M^{-1})^{ja} \quad (7)$$

Table( II) shows the inverse “sampling fractions”  $\mu_{II}^k$  for the 4 EM layers and the 1st layer of the Hadronic calorimeter. The numbers are significantly different from that in table

<i>Momentum</i>	<i>EM1</i>	<i>EM2</i>	<i>EM3</i>	<i>EM4</i>	<i>FH1</i>
	$\mu_{II}^1$	$\mu_{II}^2$	$\mu_{II}^3$	$\mu_{II}^4$	$\mu_{II}^5$
10.0	20.7	14.6	14.8	15.3	26.8
	$\mu_{II}^1$	$\mu_{II}^2$	$\mu_{II}^3$	$\mu_{II}^4$	$\mu_{II}^5$
100.0	21.8	14.6	14.7	15.6	29.1

TABLE II: Inverse “sampling fractions” method II for 10 GeV/c and 100 GeV/c electrons

(I) especially in layers 1 and 5. The numbers are obtained from a full plate simulation of the calorimeter using Geant 3.11 for 100 GeV/c electrons and invoking the above minimization algorithm.

Figure (3) is the total energy  $D^{tot}$  calculated using  $\mu_{II}$ .

The overall energy resolution in this method is better than method I by almost a factor of 2 and is equal to  $17\%/\sqrt{(E)}$ .

Since  $D^{tot} = \sum_k \mu_{II}^k L^k$ , the tendency is to assume that the deposited energy in the  $k^{th}$  layer is given by  $D^k = \mu_{II}^k L^k$ . It is the purpose of this paper to show that this assumption is false.

Figure (4) shows the difference between the calculated event by event quantities  $D^k$  using method II and the Monte Carlo measured  $D^k$  for the various layers. There is seen to be a major discrepancy between the average values and the calculated values. We explain mathematically the origin of this discrepancy in the following section.

### III. DEPOSITED ENERGY LAYER BY LAYER USING LEAST SQUARES TECHNIQUE. METHOD III

The flaw in the above argument is to assume that

$$D^k = \mu_{II}^k L^k \tag{8}$$

This equation is not general enough. The most general linear equation one can write connecting a vector  $L^k$  and another vector  $D^k$  is

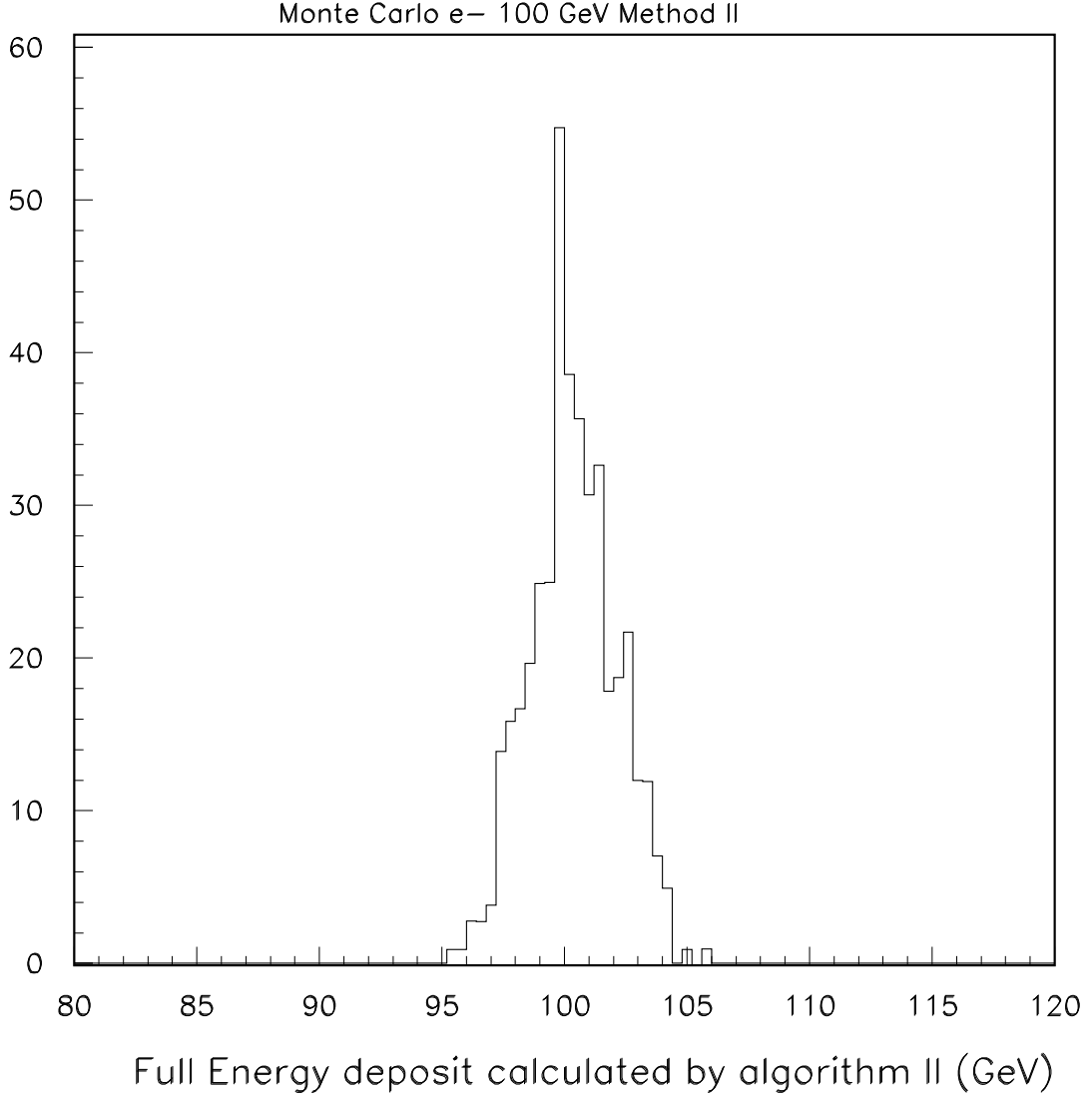


FIG. 3: Total energy of electron showers calculated using method II. The mean reconstructed energy is 99.97 GeV and the rms is 1.752 GeV

$$D^k = \sum_j \Lambda^{kj} L^j \quad (9)$$

where the tensor  $\Lambda^{kj}$  is in general non-diagonal. In the special case where it is diagonal, equation 8 results. In order to determine  $\Lambda$ , since  $D^i$  are known from Monte Carlo ,we minimize

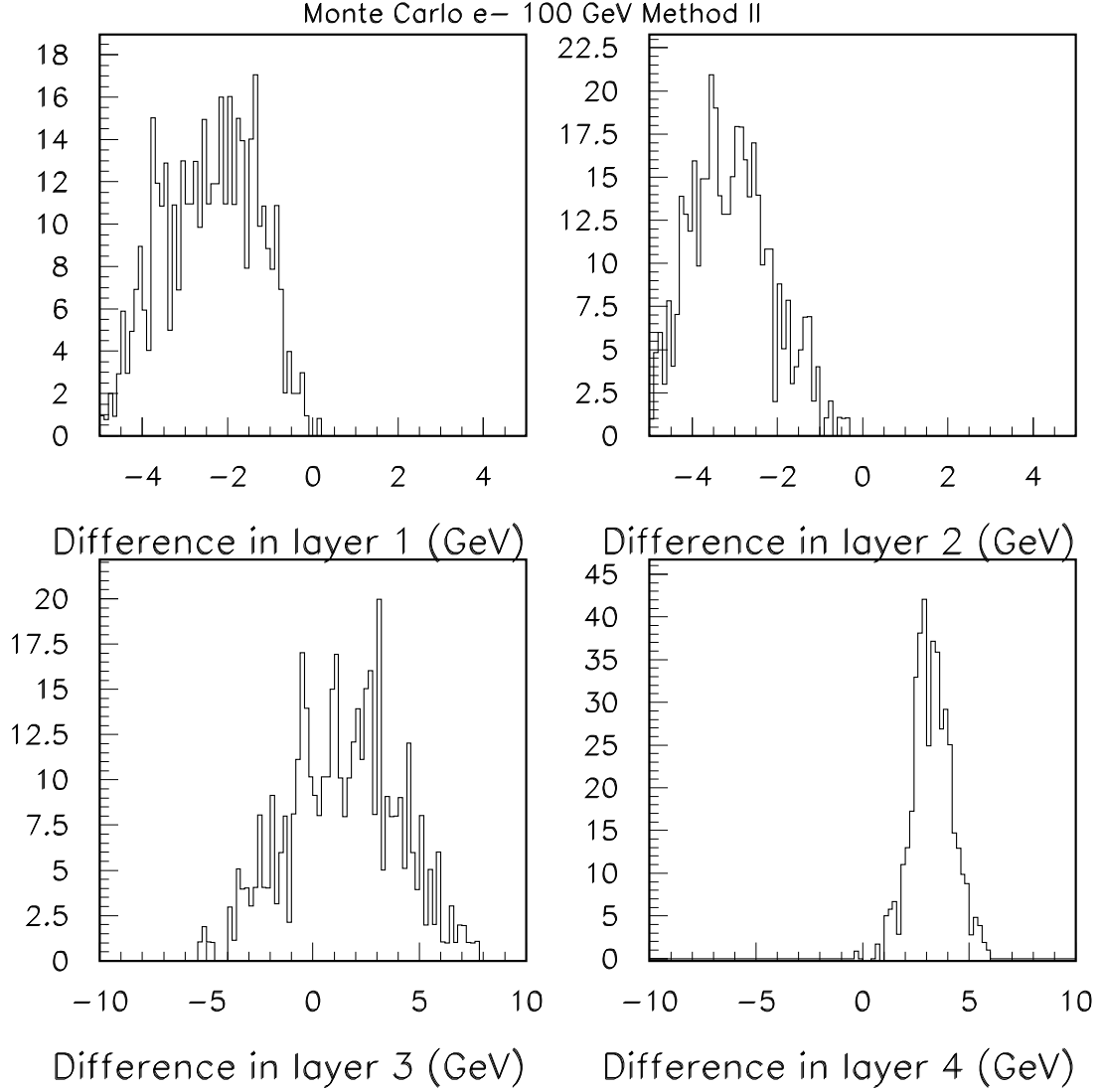


FIG. 4: Difference in calculated and measured layer by layers using method II. Layer 1 has mean,RMS of (-2.47 GeV and 1.05 GeV), layer 2 ( -3.07 GeV and 0.95 GeV), layer 3 (1.3 GeV and 2.53 GeV) and layer 4 (3.24 GeV and 0.95 GeV)

$$T^2 = \sum_{events} \sum_i (D^i - \sum_j \Lambda^{ij} L^j)^2 \quad (10)$$

yielding

$$\frac{dT^2}{d\Lambda^{ab}} = -2 \sum_{events} (D^a - \sum_j \Lambda^{aj} L^j) L^b = 0 \quad (11)$$

Averaging over events, yields

$$\langle D^a L^b \rangle = \sum_j \Lambda^{aj} \langle L^j L^b \rangle \quad (12)$$

This then yields  $\Lambda$  upon inversion

$$\Lambda^{aj} = \sum_b \langle D^a L^b \rangle (M^{-1})^{bj} \quad (13)$$

We now show that equation (12) implies equation (6). This is demonstrated by summing equation 12 over the subscript a.

$$\sum_a \langle D^a L^b \rangle = \sum_a \sum_j \Lambda^{aj} \langle L^j L^b \rangle = \langle D^{tot} L^b \rangle \quad (14)$$

But equation 6 implies that

$$\langle D^{tot} L^b \rangle = \sum_j \mu_{II}^j \langle L^j L^b \rangle \quad (15)$$

This must imply that

$$\mu_{II}^j \equiv \sum_a \Lambda^{aj} \quad (16)$$

i.e. both Method II and method III find the same minimum with the identification made in equation (16). Since the two minima are the same, it can now be seen that the energies  $D^k$  are not obtained by  $\mu_{II}^k L^k$  but are in fact obtained by equation (9).(QED). The “inverse sampling fractions ”  $\mu_{II}^k$  cannot be used to compute layer by layer energies. In order to do this one needs the full tensor  $\Lambda$ .

Table (III) gives the  $\Lambda$  tensor determined by the Least Squares Minimization . The sum of the columns of this tensor gives the same values as  $\mu_{II}$  as demanded by the mathematics.

Figure (5) shows the difference in the deposited cell by cell energies  $D^k$  computed using equation (9) and the Monte Carlo measured energies  $D^k$ . It can be seen that these predictions are far better than method II and have smaller errors than method I.

	<i>EM1</i>	<i>EM2</i>	<i>EM3</i>	<i>EM4</i>	<i>FH1</i>
<i>EM1</i>	13.2	-0.6	-0.02	-0.003	1.1
<i>EM2</i>	9.0	9.1	-0.03	-0.06	1.3
<i>EM3</i>	-4.8	7.6	13.9	-1.0	2.1
<i>EM4</i>	2.1	-1.8	1.0	15.7	-0.8
<i>EM5</i>	2.3	0.3	-0.1	0.9	25.4
<i>SUM</i>	21.8	14.6	14.7	15.6	29.1

TABLE III: The  $\Lambda$  tensor from method III for 100 GeV/c electrons

#### IV. CONCLUSION

Table (IV) summarizes the numerical results for 100 GeV/c and 10 GeV/c electrons.

To conclude, we have demonstrated that the least squares “inverse sampling fractions” cannot be used to compute cell by cell energies in the presence of correlations. This has implications when trying to compare Monte Carlo shower profiles with test beam data. In the former, both the deposited energy and the live energy is available. In the latter only the live energies are known. This paper shows that if an attempt is made to compare deposited energies between test beam data and Monte Carlo, one must use the full  $\Lambda$  tensor to infer the deposited energies. Otherwise an error is made in the shower profile which is as large as 100% in layer 1 for 100 GeV/c electrons.

Method I uses no information from shower correlations and produces a result which has a factor of 2 higher error than methods II and III for total energies. This must imply that additional information is obtained in using cell by cell correlations. It is perhaps worth pushing this question of correlations to its absolute limit and ask what the maximum attainable EM energy resolution is in a multilayer sampling calorimeter, if we had digitized information for all argon gaps independently.

#### V. ACKNOWLEDGMENTS

This work was done in 1991 when both the authors were part of the DØ collaboration. This work was performed under the auspices of the U.S. Department of Energy, by Fermi

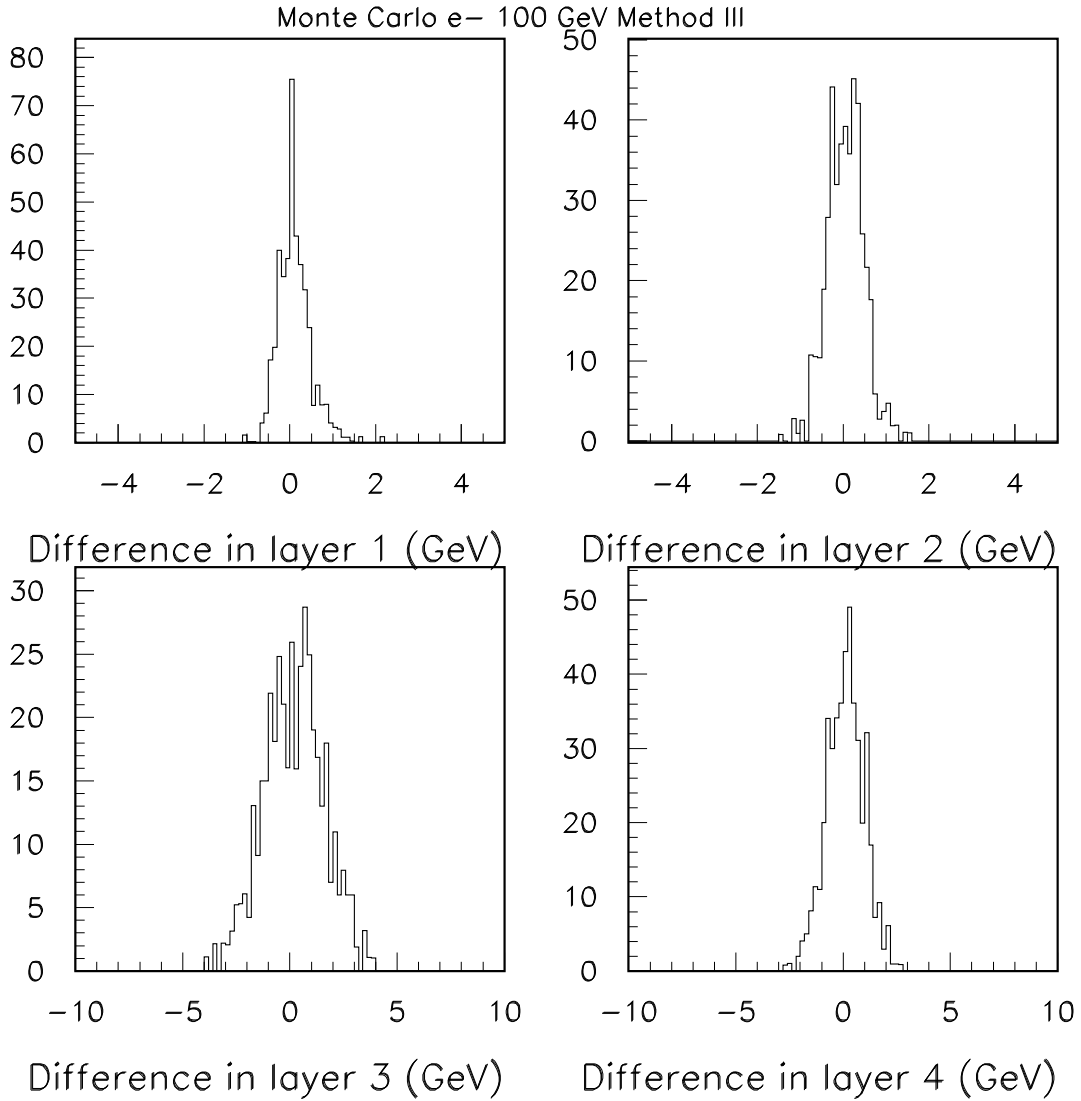


FIG. 5: Difference in calculated and measured layer by layers using method III. Layer 1 has mean,RMS of (0.13E-2 GeV and 0.375 GeV), layer 2 ( 0.18E-2 GeV and 0.42 GeV), layer 3 (0.19E-1 GeV and 1.38 GeV) and layer 4 (0.93E-2 GeV and 0.85 GeV)

National Accelerator Laboratory under Contract DE-AC02-76CH03000.

---

[1] User's Guide to GEANT 3.11, R.Brun et al, CERN DD-EE-84-1

Method	$\langle D^{tot} \rangle$	$\sigma(D^{tot})$	Deviation & Sigma deviation				
			EM1	EM2	EM3	EM4	FH1
I	9.78	0.813	$5.1E-3$	$2.5E-2$	$3.0E-2$	$1.4E-2$	$-2.7E-2$
			0.191	0.2200	0.533	0.240	0.259
II	10.01	0.588	0.4885	0.3794	-0.4418	-0.2255	-0.1898
			0.3375	0.2581	0.4809	0.2067	0.0931
$\langle L^k \rangle$			$5.719E-2$	0.156	0.376	$6.01E-2$	$0.201E-2$
$\langle D^k \rangle$			0.699	1.90	6.02	1.15	0.233
%error using methodII			70.0	20.0	-7.3	-19.6	-81.5
III	10.01	0.588	-0.0004	-0.0014	0.0014	0.0034	0.0018
			0.1899	0.1792	0.3951	0.1883	0.0506
I	100.0	4.095	$-0.6E-3$	$1.1E-3$	$1.2E-3$	$0.7E-3$	$1.3E-3$
			0.407	0.663	2.548	1.431	0.827
II	99.97	1.752	2.474	3.071	-1.302	-3.247	-1.144
			1.049	0.952	2.532	0.952	0.406
$\langle L^k \rangle$			0.225	0.905	4.26	1.15	$3.77E-2$
$\langle D^k \rangle$			2.33	10.14	64.05	21.2	2.24
%error using methodII			106.	30.3	-2.0	-15.3	-51.1
III	99.96	1.753	$-1.3E-3$	$-1.8E-3$	$-2.0E-2$	$-9.3E-3$	$2.0E-3$
			0.375	0.423	1.380	0.851	0.300

TABLE IV: Comparison summary of three methods for 10 Gev/c and 100 Gev/c electrons. Deviations here are defined as the predicted value - Monte Carlo value

[2] "The DØ detector", S.Abachi et al., Nucl. Inst. Meth. A338 (1994)p 185-253.